ARCHITECTURE OF A CHARGE-TRANSFER STATE REGULATING LIGHT HARVESTING IN A PLANT ANTENNA PROTEIN

One-sentence summary:

Regulation of photosynthetic light harvesting through thermal dissipation of excess absorbed light energy involves charge-transfer from a carotenoid to an excitonically coupled chlorophyll dimer in the CP29 pigment-protein complex of plants.

Tae Kyu Ahn,[1,2†] Thomas J. Avenson,[2,3†] Matteo Ballottari,[4] Yuan-Chung Cheng,[2] Krishna K. Niyogi, [1,3] Roberto Bassi,[4*] and Graham R. Fleming[1,2*]

[1]Physical Biosciences Division, Lawrence Berkeley National Laboratory, Berkeley, CA 94720 [2]Department of Chemistry, Hildebrand B77, University of California, Berkeley, CA 94720-1460 [3]Department of Plant and Microbial Biology, 111 Koshland Hall, University of California, Berkeley, CA 94720-3102 [4]Department of Science and Technology, University of Verona, Italy 37134

[*]To whom correspondence should be addressed: e-mail: GRFleming@lbl.gov; tel.: 510-643-3944; fax: 510-643-7012 and Bassi@sci.univr.it

[†]These authors contributed equally to this work.

Energy-dependent quenching of excess absorbed light energy (qE) is a vital mechanism for regulating photosynthetic light harvesting in higher plants. All of the physiological characteristics of qE have been positively correlated with charge-transfer between coupled chlorophyll and zeaxanthin molecules in the light-harvesting antenna of photosystem II (PSII). In this work, we present evidence for charge-transfer quenching in all three of the individual minor antenna complexes of PSII (CP29, CP26, and CP24), and we conclude that charge-transfer quenching in CP29 involves a de-localized state of an excitonically coupled chlorophyll dimer. We propose that reversible conformational changes in CP29 can 'tune' the electronic coupling between the chlorophylls in this dimer, thereby modulating the energy of the chlorophylls-zeaxanthin charge-transfer state and switching on and off the charge-transfer quenching during qE.

The photosynthetic apparatus in higher plants is designed to perform two seemingly opposing tasks: to efficiently harvest sunlight and transfer excitation energy to the reaction center (RC) but also to rapidly dissipate excessively absorbed light energy harmlessly as heat to avoid deleterious photo-damage. Because highly reactive chemical species are inevitable by-products of photosynthesis, various regulatory processes are critical for the robustness of photosynthesis and for plant survival (*1*). Regulation of light harvesting is predominantly mediated by energy-dependent quenching (qE) (*2, 3*), a phenomenon that depends on the trans-thylakoid pH gradient (ΔpH) (*4*), zeaxanthin (Z) (*5*), and the photosystem (PS) II antenna-associated protein PsbS (*6*). However, precisely how and where within PSII these components interact to mediate qE at the molecular level is still not well understood. Identification of the precise molecular architecture that

is responsible for this vital regulatory process could provide valuable insight into the design principles of photoprotection in natural photosynthesis and inspire approaches to engineer more robust artificial systems for solar energy conversion (*7-9*).

Two different mechanisms, which are not mutually exclusive, have been proposed recently to explain qE (*10, 11*). According to Ruban *et al.*, qE occurs in the peripheral, trimeric antenna of PSII called LHCII (*12*), and its molecular mechanism involves energy transfer from chlorophyll (*Chl*) *a* to a low-lying excited state of a carotenoid (lutein 1) in LHCII (*11*). A change in the conformation of a different carotenoid (neoxanthin) was identified spectroscopically and correlated with LHCII quenching *in vitro*, and this conformational change was in turn correlated with qE *in vivo* (*11*). On the other hand, we have proposed a charge-transfer (CT) mechanism for qE based on quantum chemical calculations *(13)* and ultrafast pump-probe experiments (*10, 14*). The CT mechanism involves energy transfer from the *Chls* bound to the PSII-LHCII supercomplex to a [*Chl*-*Z*] heterodimer. The [*Chl*-*Z*] heterodimer then undergoes charge separation followed by recombination, thereby transiently producing a Z radical cation ($Z^{\bullet+}$). Formation of $Z^{\bullet+}$ in thylakoids depends on the three components that are necessary for qE *in vivo* (*10, 14*). In PSII, an inner layer of monomeric (minor) antenna proteins connect the peripheral LHCII trimers to the reaction center core complex (*15, 16*). Evidence for CT quenching was recently demonstrated in a composite mixture of isolated minor antenna components (CP29, CP26, and CP24), whereas no trace of $Z^{\bullet+}$ formation signal could be found in isolated LHCII trimers (*14*). Thus, it is possible that different qE mechanisms are operating in different parts of the PSII antenna. Although each of these mechanisms has

been proposed to account fully for qE (*11, 14*), their relative contributions to qE *in vivo* remain to be determined.

To investigate the molecular architecture of CT quenching and to identify precisely which of the minor complexes are capable of mediating CT quenching, we carried out ultrafast transient absorption experiments in the spectral region of $Z^{\bullet+}$ absorption (*14, 17*) using all three of the individual, isolated minor complexes. We expressed recombinant apoproteins of CP29, CP26, and CP24 in bacteria and reconstituted them *in vitro* with *Chl*s (*a* and *b*), lutein, and either Z or violaxanthin (V). In plants and isolated thylakoids, the reversible enzymatic conversion of V to Z is correlated with qE (*5*), and previous work has shown that CT quenching is associated with the presence of Z in intact systems (*10*) and in isolated proteins (*14*), whereas V is inactive. Herein we refer to the CP29 complexes reconstituted with Z and V as CP29-Z and CP29-V, respectively (Table S1 and Fig. S1)[1]. We excited the samples at 650 nm and probed the near infrared (NIR) region where carotenoid radical cation species ($Car^{\bullet+}$) exhibit strong absorption (*10, 14*). Figure 1A shows the transient absorption profile for CP29-V as compared to that of CP29-Z. Both of which exhibit rapid rise components followed by exponential decays. However, in comparison to the CP29-V kinetics, the CP29-Z TA kinetic profile shows a larger initial amplitude rise, the component dynamics of which are clearly evident in the NIR transient absorption difference trace (Fig. 1A). For example, the difference profile is characterized by both very rapid (< 500 fs) and slower (~5.5 ps) rise components, followed by single exponential decay with a time constant of ~238 ps. Such a profile is indicative of transient $Car^{\bullet+}$ formation and is a signature of CT

[1] Materials and methods are detailed in Supporting Online Material available at Science Online

quenching (*10, 14*). The spectrum reconstructed from a series of such difference profiles obtained by probing from 880-1080 nm exhibits a broad absorption band with a maximum at ~980 nm (Fig. 1B), in good agreement with the established $Z^{\bullet+}$ absorption characteristics (*10, 14*). Similarly, the NIR transient absorption kinetics for CP26 and CP24 reconstituted with Z were also characterized by transient $Z^{\bullet+}$ formation. These combined results suggest that CT quenching, *e.g.* involving a [*Chl*-Z] species that undergoes charge separation followed by recombination, occurs within all three minor complexes. This finding is consistent with the results of genetic and spectroscopic analyses showing that no single antenna protein is specifically required for qE (*14*, *18-20*).

To further explore the molecular details of CT quenching in CP29, we studied a series of mutant CP29 complexes that each lacked a specific *Chl*. According to the previously reported homology structural model (*21, 22*), CP29 contains 8 *Chl* binding sites referred to as A1, A2, A3, A4, A5, B3, B5, and B6 and 2 carotenoid binding sites referred to as L1 and L2 (Fig. 2). Versions of CP29 with mutated ligands to each *Chl* were reconstituted *in vitro* with *Chl*s (*a* and *b*), lutein, and either V or Z, and stable complexes each lacking specific Chls were recovered except for the A1 mutant. These complexes are referred to as, for example, $CP29_{\text{-A2}}$, where the subscript denotes the missing *Chl* (Table S2 and Figs. S2-S5). Note that it is established experimentally that Z binds specifically to the L2 domain, therefore we can exclude the likelihood that *Chl* A1 is directly involved in CT quenching (*23, 24*).

The difference NIR transient absorption kinetic profile (blue trace) for $CP29_{\text{-B3}}$ is characterized by both rise and decay components that are signatures of $Z^{\bullet+}$ evolution during CT quenching (Fig. 3A), implying that CT quenching is active in the absence of

Chl B3. Likewise, the difference profiles for CP29$_{\text{-A2}}$, CP29$_{\text{-A3}}$, CP29$_{\text{-A4}}$, and CP29$_{\text{-B6}}$ also exhibit evidence of CT quenching irrespective of some variation in $Z^{\bullet+}$ signal that might derive from pleiotropic effects on protein structure (Fig. S6). These data demonstrate that CT quenching in CP29 is not eliminated by the removal of *Chl* A2, A3, A4, B3, or B6, thus excluding the likelihood of their participation in CT quenching. In contrast, the kinetic profiles for CP29$_{\text{-A5}}$, whether reconstituted with Z or V, are characterized solely by decay features attributable to *Chl* excited state absorption, and the transient absorption difference profile reveals no significant amplitude change relative to the noise level (Fig. 3B). The interpretation of this result is complicated by the fact that mutation of the amino acid residue that coordinates *Chl* A5 also results in the loss of *Chl* B5, specifically in Z-bound CP29 complexes (Table S2). However, the kinetic profiles for CP29$_{\text{-B5}}$ (a complex lacking *Chl* B5 only) are also characterized solely by *Chl* excited state absorption dynamics and no measurable $Z^{\bullet+}$ formation signal (Fig. 3C), which clearly indicates that CT quenching in CP29 involves *Chl* B5. According to the homology structural model (Fig. 4), *Chl* B5 is placed further away from Z (~13**Å**) than is *Chl* A5 (~6**Å**). The *Chl*s A5/B5 pair is positioned within the L2 domain and *Chl* A5 is orientated roughly co-facial to, and centered along the axis of, the Z binding site, which is in good agreement with the requirements for CT quenching previously predicted by quantum chemistry calculations (*13*). Furthermore, *Chl*s A5 and B5 are reported to be strongly coupled (*22, 25*), and both are important for the regulation of *Chl* excited states (*21, 22*). Therefore, we conclude that CT quenching in CP29 most likely depends on both *Chl*s A5

and B5, and rather than a simple [*Chl*-*Z*] heterodimer, the molecular site of CT quenching in CP29 is comprised of Z and a strongly coupled *Chl* pair (A5 and B5).

What is the significance of this CT site architecture? Our finding indicates that the primary event of CT quenching in CP29 involves electron transfer from Z to a strongly coupled *Chl* dimer in the A5/B5 pocket of CP29, rather than from Z to a monomeric *Chl* molecule (*26*). A coupled *Chl* dimer, compared to a monomeric *Chl*, would be more favorable for CT quenching because the charge delocalization over the two *Chl*s will make the product CT state more stable. As a result, controlling the coupling strength between *Chl*s A5 and B5 in CP29, either by changing the distance between them or by altering their orientations, would modulate the reduction potential of the *Chl* dimer and therefore could be used to switch on and off the CT quenching. This CT switching mechanism provides a potential molecular basis for the regulation of CT quenching during qE in the higher plant antenna.

The rapid reversibility of qE at the physiological level is thought to result from changes in the trans-thylakoid ΔpH that occurs, for example, during fluctuations in incident solar flux density. It has been proposed that two thylakoid lumen-exposed glutamate residues of the PsbS protein sense these changes in pH (*27*) and induce protein conformational changes that control qE. Moreover, PsbS has recently been shown not to bind pigments (*28*) but to interact with CP29 (*29*). Therefore, we propose that pH-dependent protein conformational changes that are transduced from PsbS to CP29 (and possibly other minor antenna complexes) can alter the coupling strength between *Chl*s A5 and B5 in CP29 and induce CT quenching during qE. Experiments that can directly probe

the efficiency of CT quenching while modulating the electronic coupling between *Chl*s A5 and B5 can test this proposal.

Converging results based on theoretical calculations, molecular genetic analysis, and ultrafast spectroscopy have shown that the mechanism involving CT quenching in minor complexes is emerging as a key component of qE. Our results show that CT quenching can occur in all three minor antenna complexes, which are positioned between LHCII and the RC, a perfect setting for regulating excitation energy transfer to the RC.

REFERENCES AND NOTES

1. C. Kulheim, J. Agren, S. Jansson, *Science* **297**, 91 (2002).
2. P. Horton, A. V. Ruban, R. G. Walters, *Annu. Rev. Plant Phys.* **47**, 655 (1996).
3. K. K. Niyogi, *Annu. Rev. Plant Phys.* **50**, 333 (1999).
4. J. M. Briantais, C. Vernotte, M. Picaud, G. H. Krause, *Biochim. Biophys. Acta* **548**, 128 (1979).
5. B. Demmig-Adams, *Biochim. Biophys. Acta* **1020**, 1 (1990).
6. X.-P. Li *et al.*, *Nature* **403**, 391 (2000).
7. R. Berera *et al.*, *Proc. Natl. Acad. Sci. U. S. A.* **103**, 5343 (2006).
8. A. Hagfeldt, M. Gratzel, *Acc. Chem. Res.* **33**, 269 (2000).
9. T. A. Moore, A. L. Moore, D. Gust, *Philos. Trans. R. Soc. B-Biol. Sci.* **357**, 1481 (2002).
10. N. E. Holt *et al.*, *Science* **307**, 433 (2005).
11. A. V. Ruban *et al.*, *Nature* **450**, 575 (2007).

12. Z. F. Liu *et al.*, *Nature* **428**, 287 (2004).

13. A. Dreuw, G. R. Fleming, M. Head-Gordon, *Phys. Chem. Chem. Phys.* **5**, 3247 (2003).

14. T. J. Avenson *et al.*, *J. Biol. Chem.* **283**, 3550 (2008).

15. E. J. Boekema *et al.*, *Proc. Natl. Acad. Sci. U. S. A.* **92**, 175 (1995).

16. K. H. Rhee *et al., Nature* **389**, 522 (1997).

17. S. Amarie *et al.*, *J. Phys. Chem.B* **111**, 3481 (2007).

18. J. Andersson, R. G. Walters, P. Horton, S. Jansson, *Plant Cell* **13**, 1193 (2001).

19. J. Andersson *et al.*, *Plant J.* **35**, 350 (2003).

20. L. Kovacs *et al.*, *Plant Cell* **18**, 3106 (2006).

21. R. Bassi, R. Croce, D. Cugini, D. Sandona, *Proc. Natl. Acad. Sci. U. S. A.* **96**, 10056 (1999).

22. G. Cinque, R. Croce, A. Holzwarth, R. Bassi, *Biophys. J.* **79**, 1706 (2000).

23. J. P. Connelly *et al.*, *Biochemistry* **36**, 281 (1997).

24. T. Morosinotto, S. Caffarri, L. Dall'Osto, R. Bassi, *Physiol. Plant.* **119**, 347 (2003).

25. H. van Amerongen, R. van Grondelle, *J. Phys. Chem. B* **105**, 604 (2001).

26. Formation of a delocalized *Chl* dimer would depend on occupancy of both A5 and B5 sites by *Chl a.* Although the A5 site exclusively binds *Chl a*, B5 is a mixed site of *Chl*s *a* and *b* in minor complexes (CP29, CP26, and CP24) (*19*). Therefore, a delocalized *Chl a* dimer can form within the A5 and B5 sites in CP29. Moreover, this dimer structure could also explain why $Z^{\bullet+}$ formation is not favored in LHCII (*14*), in which the A5 and B5 sites bind specifically *Chl*s *a* and *b,* respectively (*12*). Because the large spectral

absorbance gap (ca. 700 cm^{-1}) between *Chl*s *a* and *b* prohibits the delocalization over the a *Chl* heterodimer, no CT state can be produced in L2 site of LHCII. One additional factor of specificity is that the capacity of LHCII to undergo exchange of V to Z in site L2 *in vivo* is very low compared to minor complexes (*22*).

27. X.-P. Li *et al.*, *J. Biol. Chem.* **279**, 22866 (2004).

28. G. Bonente *et al.*, *J. Biol. Chem.* **283**, 8434 (2008).

29. E. Teardo *et al.*, *Biochim. Biophys. Acta* **1767**, 703 (2007).

30. We thank Dr. Donatas Zigmantas for helpful discussions. This work was supported by the Korea Research Foundation Grant (KRF-2006-214-C00037) funded by the Korean Government (MOEHRD) (T.K.A.), the National Research Initiative Competitive Grant (2006-03279) (T.J.A.), This work was also supported by the Director, Office of Science, Office of Basic Energy Sciences, of the U.S. Department of Energy under Contract No. DE-AC02-05CH11231 and by the Chemical Sciences, Geosciences and Biosciences Division, Office of Basic Energy Sciences, U.S. Department of Energy under contract DE-AC03-76SF000098 (G.R.F. and K.K.N). R.B. thanks to the FIRB contract RBLA0345SF from the Italian Basic Research Foundation and contract SAMBA Trento Research Council for foundational support.

Supporting Online Material

www.sciencemag.org

Materials and Methods

Tables. S1, S2

Figs. S1, S2, S3, S4, S5, S6

SOM References

FIGURE LEGENDS

Figure 1. NIR TA kinetics for the CP29 minor complexes probed at 980 nm. (A) NIR transient absorption profiles for isolated CP29 complexes with excitation at 650 nm (*Chl b* Q_y transition) and probing at 980 nm. The red and black profiles represent kinetics for CP29 complexes bound by Z and V, respectively. Note that the samples are prepared so that they have the same absorbance (0.3) at 650 nm, and these kinetic traces have not been normalized in any way. The difference kinetic trace (blue curve) is obtained by subtraction of the V-kinetic profiles from the Z-kinetic profiles. Inset: transient absorption profiles over a shorter time region (0-60 ps). (B) NIR transient absorption spectrum for the isolated CP29 complexes. The spectrum was constructed from a series of NIR transient difference profiles obtained 15 ps after excitation by probing every 20 nm from 880 to 1080 nm. Error bars represent the standard error (SE) of five trials. The solid curve represents a b-spline interpolation among the experimental data points.

Figure 2. CP29 homology structure model. The model shows eight *Chl*s and two carotenoid binding sites (L1 and L2). The structure was constructed based on homology data, mutational analyses, circular dichroism, and spectroscopic results (*19, 20*). *Chl*s A1 and A2 are located in the L1 carotenoid binding pocket, whereas *Chl*s A4, A5, B5, B6 are close to the L2 site.

Figure 3. NIR transient absorption kinetics for CP29 mutants lacking the ligands binding to *Chl*s B3, A5, and B5. Transient absorption profiles were measured using $CP29_{-B3}$ (A), $CP29_{-A5}$ (B), $CP29_{-B5}$ (C). Other conditions are the same as Fig. 1A.

Figure 4. Molecular details of the CT quenching site in CP29. Molecular sites responsible for CT quenching in CP29, including the Z bound in the L2 site and *Chl*s A5 and B5 are shown. Based on the homology model, the center-center distances for *Chl* A5 to Z, *Chl*s A5 to B5, and *Chl* B5 to Z, are estimated to be ~6**Å**, ~10**Å**, and ~13**Å**, respectively. The dihedral angle between *Chl*s A5 and B5 is about 41°. The structure indicates that *Chl*s A5 and B5 are strongly coupled to each other.

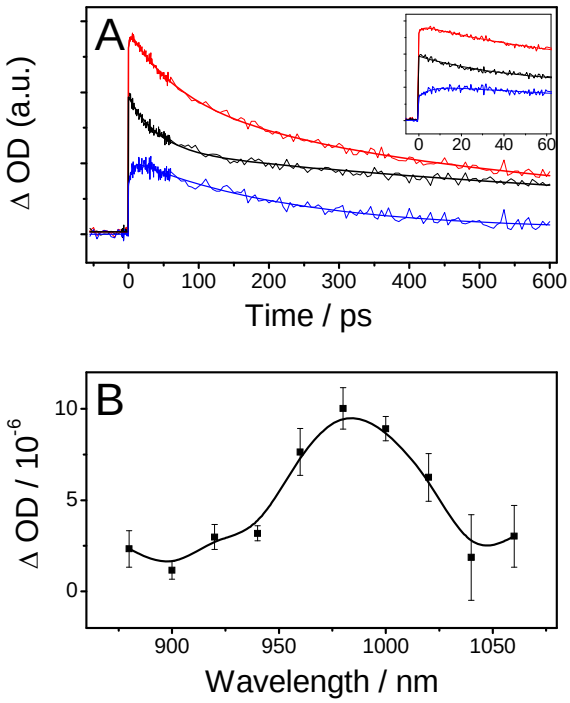
A
Δ OD (a.u.)
0
100
200
300
400
500
600
Time / ps
0
20
40
60
B
Δ OD / 10^-6
10
5
0
900
950
1000
1050
Wavelength / nm

Figure 1

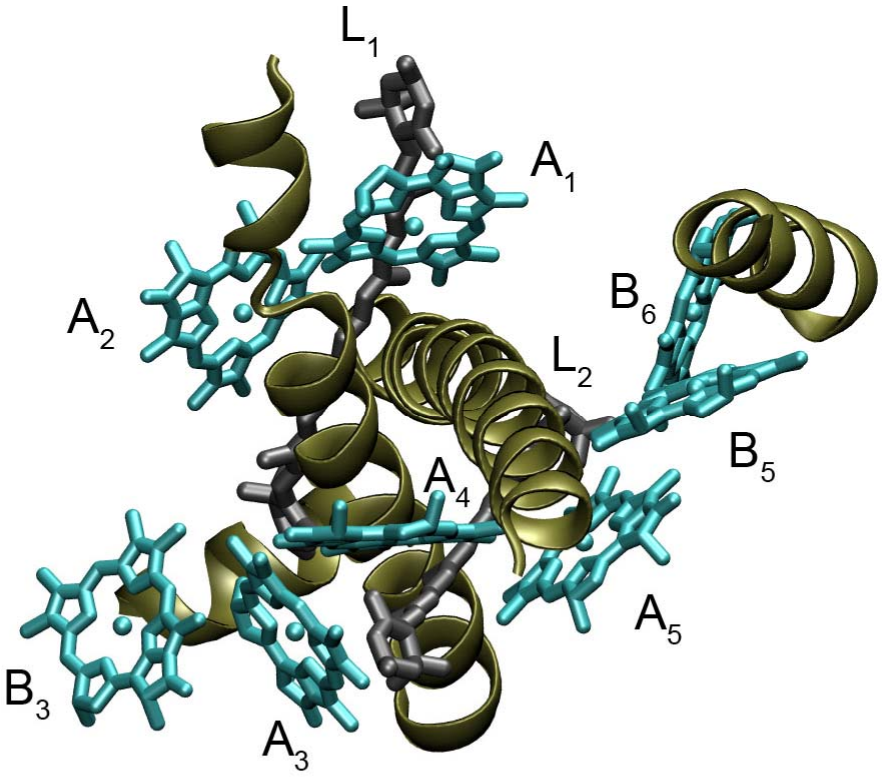

Figure 2

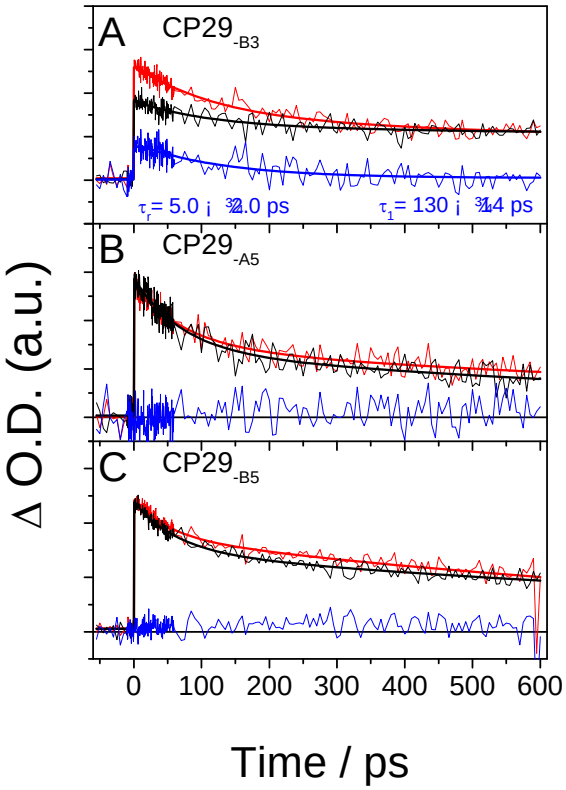
A
CP29-B3
B
CP29-A5
C
CP29-B5
Δ O.D. (a.u.)
0
100
200
300
400
500
600
Time / ps

Figure 3

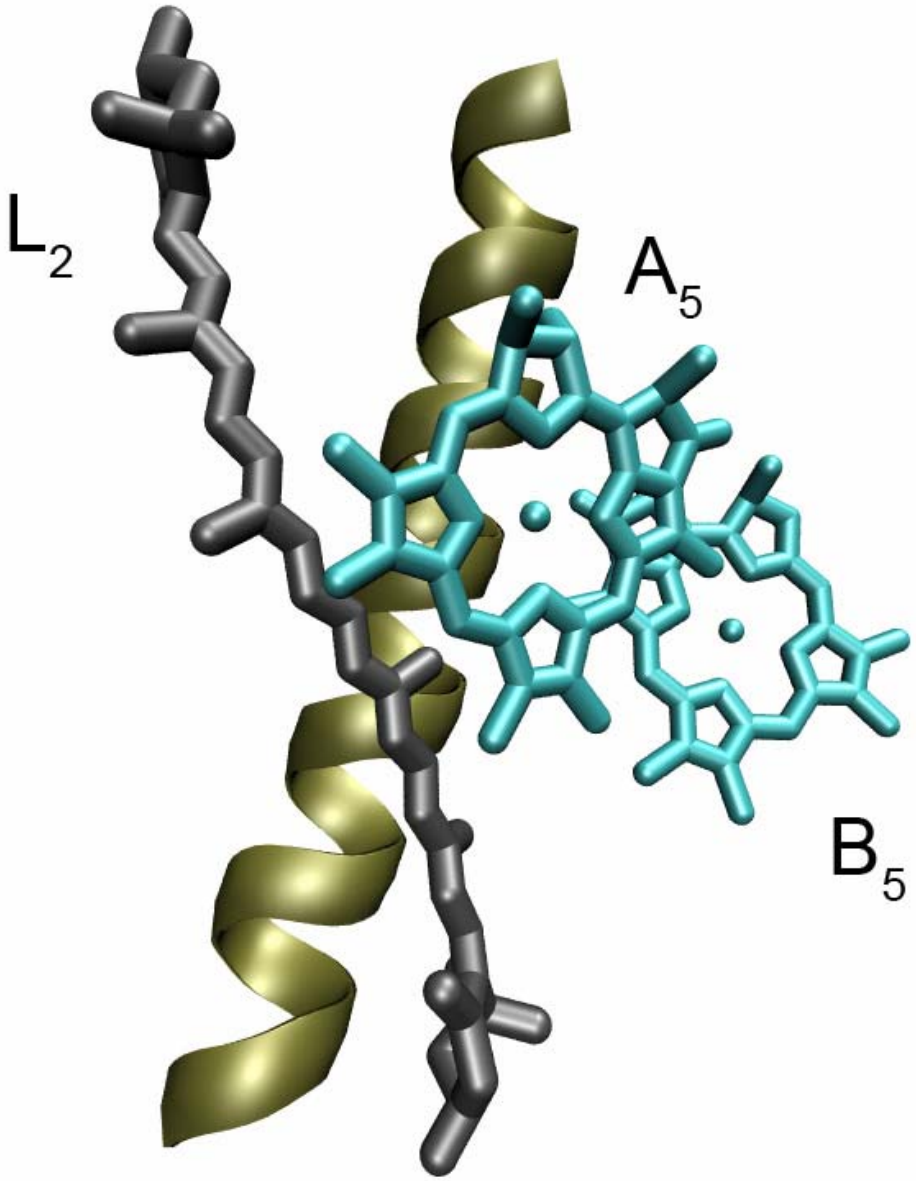

Figure 4

–

Supporting Online Material

MATERIALS AND METHODS

Preparation and characterization of wild-type and mutant antenna complexes with specific xanthophylls.

The *lhcb4*, *lhcb5*, and *lhcb6* genes from *Arabidopsis thaliana* and for the monomeric polypeptides CP29, CP26, and CP24, respectively, were individually expressed in *E. coli*, and the apoproteins were isolated, followed by *in vitro* reconstitution with *Chl*s (*a* and *b*), lutein and either V or Z, essentially as previously reported (*S1*). Mutations of *Chl* binding residues were as in (*S2*).

The compositions and properties of the recombinant wild-type (WT) and mutant complexes were confirmed by pigment analysis (Table S1) and absorption spectroscopy (Fig. S1). Pigments were extracted from the isolated antenna complexes with 80% acetone, then separated and quantified by HPLC as described in (*S3*) and by fitting analysis of the spectrum of the acetone extract with the spectra of individual pigments as described in (*S4*). Refolded monomeric complexes were re-suspended in buffer solution (5 mM HEPES and 0.06% α-DM at pH 7.6) to an OD of ~0.3/mm at 650 nm for transient absorption analyses.

NIR transient absorption

The NIR transient absorption laser system has been previously described (*S5, S6*). Briefly, the repetition rate was 250 kHz and the pump pulses were tuned to ~650 nm (i.e.

the *Chl b* Q_y transition). The maximum pump energy and FWHM of the pulse auto-correlation trace were ~48 nJ/pulse and ~40 fs, respectively. We chose 650 nm as our excitation wavelength because the output power of our OPA was higher there than that at 680 nm, yielding higher signal:noise ratios. *Chl b* to *a* energy transfer occurs on the 100-200 fs and tens of ps timescale (*S7*), making results on the timescale studied here insensitive to whether *Chl b* or *Chl a* is initially excited. White light continuum probe pulses were generated in a 1 mm quartz plate. The observation of the cross-correlation function of the pump and probe overlap was ca. 85 fs. The diameters of the pump and probe beams at the sample holder were 141 μm and 81 μm, respectively. The mutual polarizations of the pump and probe beams were set to the magic angle (54.7°). The time resolution of our transient absorption measurements was 5ps/point (-60 ps to -10 ps), 0.5 ps/point (-10 ps to 60 ps), and 5 ps/point (65 ps to 600 ps). A monochromator (Spectra Pro 300i, Acton Research Corp., Acton, MA) and a InGaAs photodiode (DET410, Thorlabs, Newton, NJ) were used to monitor transmission. A sample cell for isolated LHCs with a path length of 1 mm was chilled by a circulating water bath (VWR Scientific 1160, PolyScientific, Niles, IL) which was set at 7°C during the data acquisition to prevent sample degradation.

Characterization of minor antenna complexes (CP29, CP26, and CP24).

Table S1. Pigment analysis of minor antenna complexes (CP29, CP26, and CP24) reconstituted in the presence of V (CP-V) or Z (CP-Z).

Sample	No. *Chl*[1]	*Chl a*/*b*[2]	*Chl* /car[3]	Neo[4]	V[5]	Anthera[6]	Lutein[7]	Z[8]	β-car[9]	No. Car[10]
CP29-V	**8.0**	**3.1**	**4.1**	**0.5**	**0.5**	**0.0**	**1.0**	**0.0**	**0.0**	**2.0**
CP29-Z	**8.0**	**2.9**	**4.4**	**0.0**	**0.0**	**0.0**	**0.9**	**1.0**	**0.0**	**1.9**
CP26-V	**9.0**	**2.2**	**3.5**	**0.8**	**0.2**	**0.0**	**1.6**	**0.0**	**0.0**	**2.6**
CP26-Z	**9.0**	**2.0**	**4.2**	**0.0**	**0.0**	**0.0**	**1.1**	**1.1**	**0.0**	**2.1**
CP24-V	**10.0**	**1.5**	**4.4**	**0.0**	**0.6**	**0.0**	**1.6**	**0.0**	**0.0**	**2.2**
CP24-Z	**10.0**	**1.6**	**4.7**	**0.0**	**0.0**	**0.0**	**0.8**	**1.4**	**0.0**	**2.1**

[1]Total number of *Chl*s per complex.

[2]The ratio of *Chl a* divided by *Chl b* per complex.

[3]The ratio of *Chl*s divided by total carotenoid per complex.

[4]The number of neoxanthin per complex.

[5]The number of V per complex.

[6]The number of antheraxanthin per complex.

[7]The number of lutein per complex.

[8]The number of β-carotene per complex.

[9]The number of Z per complex.

[10]The total number of carotenoid per complex.

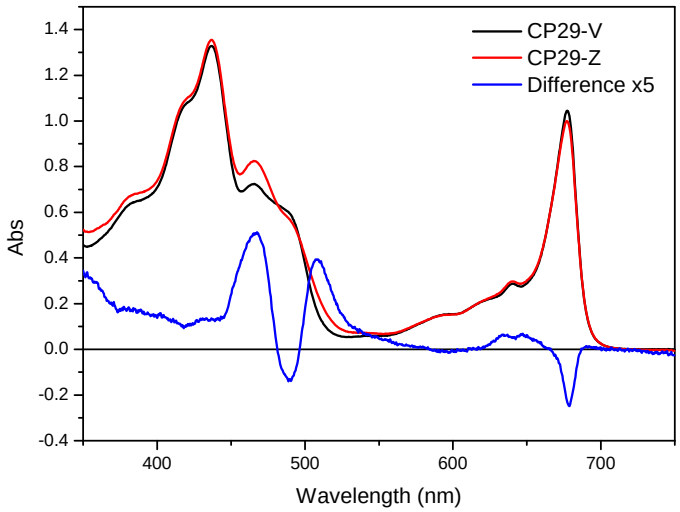

Figure S1. Steady-state absorption spectra of CP29-Z and –V complexes. Differences were observed both in the Soret region due to the direct absorption of xanthophylls and in the Q_y transition region. Since carotenoids do not absorb in the 600-700 nm range, the differences in the Q_y region are due to changes in the protein-*Chl* interaction induced by Z-dependent conformational changes.

Characterization of CP29 mutants.

Table S2. Pigment analysis of CP29 mutants with Z in the *Chl* binding sites.[1]

Sample	No. *Chl*	*Chl a*/*Chl b*	*Chl* /Car	No. Car	Lutein	Z	*Chl a*	*Chl b*	Δ *Chl* a^2	Δ *Chl* b^2
Wild-type	8	2.90	4.3	1.9	1.2	0.7	5.9	2.1	0.00	0.00
[3]**CP29$_{\text{-A2}}$**	7	2.72	4.0	1.8	1.2	0.6	5.1	1.9	0.90	0.10
CP29$_{\text{-A3}}$	7	3.47	4.8	1.5	1.0	0.4	5.4	1.6	0.52	0.48
CP29$_{\text{-A4}}$	7	2.89	5.0	1.4	1.0	0.4	5.2	1.8	0.75	0.25
CP29$_{\text{-A5}}$	6	2.69	4.1	1.5	1.0	0.4	4.4	1.6	1.57	0.43
CP29$_{\text{-B3}}$	7	3.53	4.1	1.7	1.2	0.5	5.5	1.5	0.50	0.50
CP29$_{\text{-B5}}$	7	3.93	5.4	1.3	0.9	0.4	5.6	1.4	0.37	0.63
CP29$_{\text{-B6}}$[4]	8	3.46	4.7	1.7	1.2	0.5	6.2	1.8	-0.26	0.26

[1]The specific details of CP29 mutants with V was described in (*S2*). The A3, B3, B5, and B6 sites are mixed sites that can bind either *Chl a* or *b*, resulting in an average *Chl* composition of 5.6 *Chl*s *a* and 2.4 *Chl*s *b* in CP29 (*S8*). Z binds specifically to the L2 domain (*S9, S10*).

[2]Δ *Chl* indicates the change of numbers of *Chl*s.

[3]CP29$_{\text{-A1}}$ was unable to refold with pigments (*S2*).

[4]The mutation for CP29$_{\text{-B6}}$ does not remove *Chl* B6 but changes the chromophore to *Chl b*, which cannot undergo electron transfer with Z and is therefore equivalent to a deletion as far as CT is concerned.

Characterization of CP29$_{-A5}$ with Z

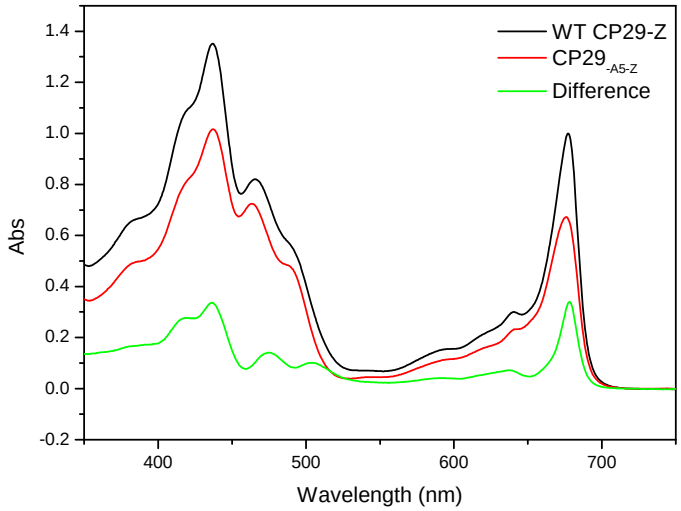

Figure S2. Steady-state absorption spectra of A5 mutants reconstituted with Lut and Z compared with the WT spectrum. Differences were observed both in the Soret region due to the direct absorption of xanthophylls and in the Q_y transition region. The differences in the Q_y region are specifically due to the lack of *Chl*s A5 and B5.

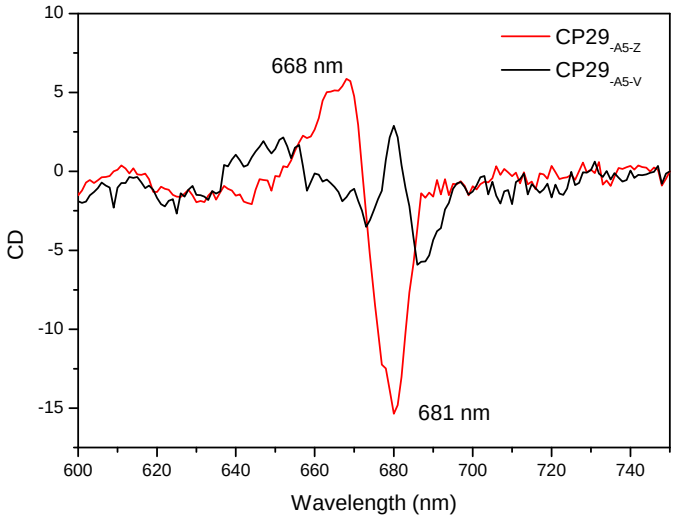

Figure S3. Circular Dichroism (CD) difference spectra (CP29 WT minus CP29$_{-A5}$) of complexes with Z (red) and with V (black). Mutation at *Chl* A5 binding site induces loss of a conservative signal with terms at 668 (+) and 681 nm (-) in Z binding but not in V binding complexes. This result implies that binding of Z induces a conformational change establishing an excitonic interaction with a second *Chl* molecule, previously not evident. According to the structural model, the only possible partner for this interaction is *Chl* B5.

Characterization of CP29$_{-B5}$ with Z

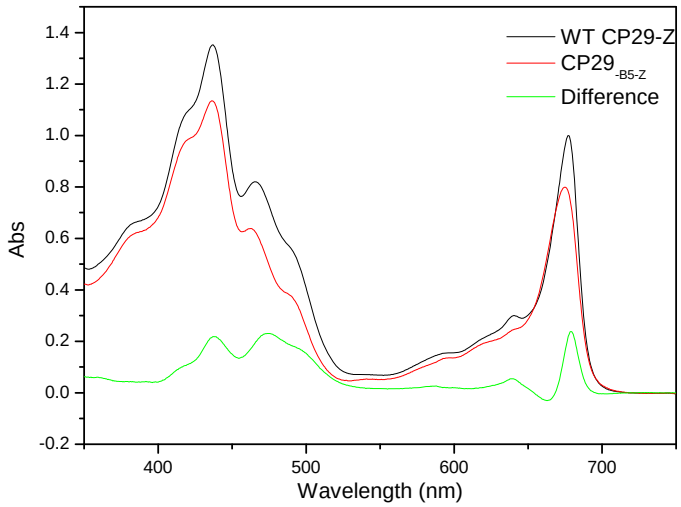

Figure S4. Steady-state absorption spectra of B5 mutants compared with that of WT CP29. Both proteins were reconstituted with L + Z. Differences were observed both in the Soret region due to the direct absorption of xanthophylls and in the Q_y transition region. The differences in the Q_y region are specifically due to the lack of *Chl* B5.

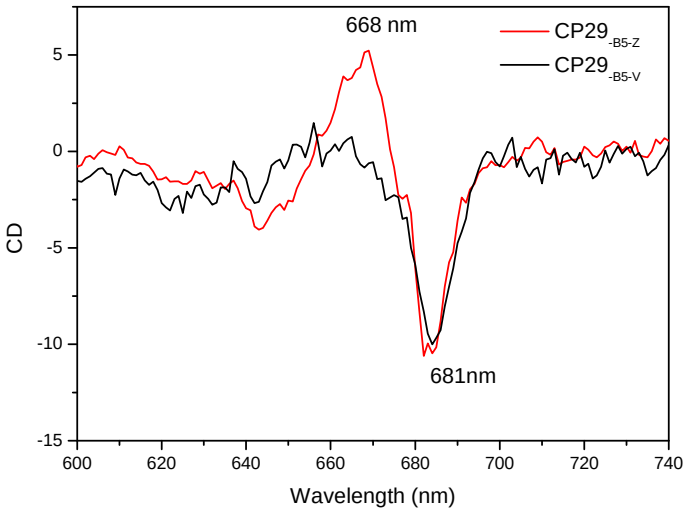

Figure S5. CD difference spectra (CP29 WT minus CP29$_{-B5}$) of complexes with Z (red) and with V (black). Mutation at *Chl* B5 binding site induces loss of a conservative signal with terms at 668 (+) and 681 nm (-) in Z binding but not in V binding complexes. This result implies that binding of Z induces a conformational change establishing an excitonic interaction with a second *Chl* molecule, previously not evident. The interaction is the same as shown upon deletion of *Chl* A5 (see above) implying that *Chl* A5 and *Chl* B5 undergo excitonic interaction.

Kinetic profiles of CP29$_{-A2}$, $_{-A3}$, $_{-A4}$, and $_{-B6}$.

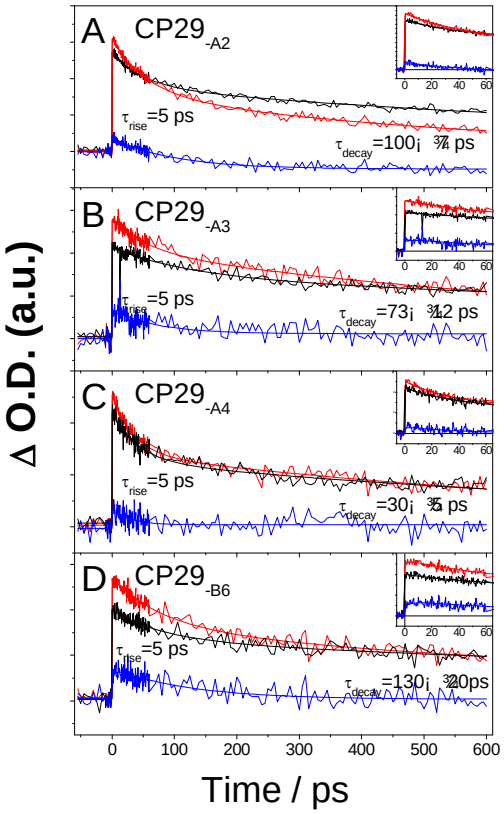

Figure S6. NIR transient absorption kinetics for CP29 lacking the ligands for *Chl*s A2, A3, A4, and B6. Kinetic profiles from probing at 980 nm were obtained using CP29$_{-A2}$ (A), CP29$_{-A3}$ (B), CP29$_{-A4}$ (C), and CP29$_{-B6}$ (D). Inset: transient absorption profiles over the 0-60 ps time region. Other conditions are the same as for Fig. 1A in the main text. The red and black profiles represent TA kinetics for the corresponding complexes bound by Z and V, respectively. Difference kinetic traces (blue) correspond to subtraction

of the V-kinetic profiles from the Z-kinetic profiles. The V-bound complexes show solely decay components which correspond to *Chl* excited state absorption, whereas the Z-bound complexes reveal ultrafast rise and moderate decay components. The difference profiles of CP29 mutants exhibit 5-ps rise components and around 100-ps decay components, implying the generation of $Z^{\bullet+}$, a signature of CT quenching. The variable decay time constants for the respective difference profiles likely originate from heterogeneity of protein environments that surround the CT state.

SOM References

S1. E. Giuffra, D. Cugini, R. Croce, R. Bassi, *Eur. J. Biochem.* **238**, 112 (1996).

S2. R. Bassi, R. Croce, D. Cugini, D. Sandona, *Proc. Natl. Acad. Sci. U. S. A.* **96**, 10056 (1999).

S3. A. M. Gilmore, H. Y. Yamamoto, *Plant Physiol.* **96**, 635 (1991).

S4. R. Croce, G. Canino, F. Ros, R. Bassi, *Biochemistry* **41**, 7334 (2002).

S5. T. J. Avenson *et al.*, *J. Biol. Chem.* **283**, 3550 (2008).

S6. N. E. Holt *et al.*, *Science* **307**, 433 (2005).

S7. V. Barzda *et al.*, *Biophys. J.* **80**, 2409 (2001).

S8. G. Cinque, R. Croce, A. Holzwarth, R. Bassi, *Biophys. J.* **79**, 1706 (2000).

S9. J. P. Connelly *et al.*, *Biochemistry* **36**, 281 (1997).

S10. T. Morosinotto, S. Caffarri, L. Dall'Osto, R. Bassi, *Physiol. Plant.* **119**, 347 (2003).